ELSEVIER

Journal of Geochemical Exploration 74 (2001) 73–97

JOURNAL OF GEOCHEMICAL EXPLORATION

www.elsevier.com/locate/jgeoexp

Hydrochemical modelling for preliminary assessment of minewater pollution

Steven A. Banwart[a,*], Maria E. Malmström[b]

[a]*Department of Civil and Structural Engineering, The University of Sheffield, Mappin Street, Sheffield S1 3JD, UK*
[b]*Department of Civil and Environmental Engineering, The Royal Institute of Technology, Stockholm, Sweden*

Received 5 September 1999; accepted 14 October 2000

Abstract

A conceptual model for preliminary assessment of minewater pollution within the risk-based corrective action (RBCA) framework for environmental management is developed. The model aims to assist classification of a site regarding the potential threat to the environment and help assess whether the assumptions used in this classification are appropriate. The model estimates contamination source strength, longevity and possible future changes in discharge quality and can be applied with sparse data sets. The model relates solute export in the discharge to source minerals which includes sulphide phases that produce acidity and metals contamination and carbonate and aluminosilicate phases which provide natural attenuation to neutralise acidity and immobilise metals.

We present and apply limited data from three sites representing a mine rock waste deposit located above the water table, a flooded abandoned coal mine with deep workings and a mine tailings deposit. Results from the rock waste deposit indicate that calcite no longer provides significant attenuation of the present acidity load and that acid generation and associated loads of Cu^{2+} may persist for a period of up to two centuries. The abandoned coal mine has a discharge that is presently alkaline, with calcite depletion expected to occur before pyrite is consumed, possibly yielding a future drop in pH. The lifetime for these minerals is similar at this site, and on the order of several centuries, thus rendering the estimate of future water quality evolution very uncertain. The mill tailings deposit is expected to produce acidic discharge on a time scale of one century. However, conclusive quantification of calcite weathering was not possible, leaving open the possibility that the weathering of Mg-silicate minerals provides important attenuation of the present acidity load.

Keywords: hydrochemical modelling; minewater; pollution; risk assessment

1. Introduction

Modern mining methods have world wide lead to rapidly increasing volumes of mine wastes in the form of both waste rock, normally deposited in waste rock piles, and mill tailings, deposited in impoundments. During thousands of years of mining, a large number of mine sites have been abandoned and open pits and underground mines have been left unattended. The exposed material often contains significant amounts of elements in their reduced state that are readily oxidised by available oxidants, such as dissolved oxygen and oxygen in the pore gas as well as ferric iron. Such oxidative weathering of various sulphide minerals may result in the generation of acid mine drainage (AMD), characterised by net acidity and high concentrations of dissolved, hazardous metals, e.g. Cu^{2+}, Zn^{2+}, metalloids, e.g. As, and sulphate.

* Corresponding author. Tel.: +44-114-222-5742; fax: +44-114-222-5700.
E-mail address: s.a.banwart@sheffield.ac.uk (S.A. Banwart).

0375-6742/01/$ - see front matter
PII: S0375-6742(01)00176-5

Whether or not a particular site will produce such leachates depends in part on the natural capacity to attenuate released acidity, metalloids and metals. A key parameter that determines the environmental risk associated with mine sites is the drainage pH, as low pH normally is connected to high metal concentrations and mobility. Today, a great number of mine- and mine waste sites around the world are already producing acidic leachates, and yet others remain as potential, future environmental threats. The mining industries and environmental protection agencies are hence faced with risk assessments and decision-making regarding potential treatment options at numerous sites. Common methods to assess mine sites include site observations and tests, laboratory tests (static tests, see e.g. White et al. (1999) and kinetic tests, see e.g. White and Jeffers (1994)), and geochemical modelling (see e.g. Perkins et al. (1997) and Alpers and Nordstrom (1999)). Recently, Paktunc (1999a,b) suggested a method to predict AMD from the mineralogical composition of the material.

Within the framework of Risk-Based Corrective Action (RBCA; see e.g. ASTM, 1995), the decision process for site remediation is organised into a hierarchy of increasingly complex assessments that apply the Source–Pathway–Target risk assessment methodology. Initial site assessment identifies possible contamination sources, transport pathways and sensitive targets such as surface waters or groundwater wells. Initial assessment classifies sites, for example into those representing (1) an immediate threat requiring remediation, (2) a short-term threat (for example, <2 years), (3) a long-term threat (>2 years) or (4) no perceived threat. A 'Tier 1' evaluation then identifies exposure routes and scenarios (concentration, timing and duration of exposure) and compares these scenarios with conservative parameters. An example would be to use drinking water standards for contaminant concentrations as a decision basis for remediation; under the extremely conservative assumption that the discharge from the site will be used directly for water supply. Important decision factors at Tier 1 include determining (1) if the assumptions used to classify the site and assign remedial action (or not) are appropriate for conditions at the site, (2) the cost of corrective action to acceptably reduce the threat, (3) the cost of moving to higher-tiered, more detailed risk assessment (data collection, analysis, predictive modelling, etc.) and (4) the likelihood that a higher-tiered assessment will result in a significantly different classification of the site and assigned remedial action. Decisions at Tier 1 thus include (1) screen out site (no further action), (2) design a remediation plan, (3) an interim response action or (4) a Tier 'upgrade'. Upgrade to Tier 2 commonly includes applying the Tier 1 parameters at alternative compliance points. For the example of using drinking water standards, these could be applied to an abstraction point downstream of the discharge where significant dilution has occurred due to mixing of the discharge in the receiving stream. Also, site-specific fate and transport modelling can be carried out and, if appropriate, a statistical representation of site characterisation data may be used. A tier upgrade is generally associated with additional site characterisation work such as water quality sampling, borehole investigations, hydrological monitoring and mineralogical studies.

The possible decisions after assessment at Tier 2 are the same as for Tier 1. In this case, an upgrade to Tier 3 involves the highest level of sophistication and may include development of new site-specific numerical models, detailed site investigation for spatial resolution of site properties, use of stochastic modelling, etc. Because this level of analysis is highly specialised, the associated costs to carry out the assessment are also much higher than for the lower levels of assessment.

For the Aitik site described below, further investigations (corresponding to Tier 3) included geochemical (Strömberg and Banwart, 1994) and reactive transport (Eriksson et al., 1997) modelling, static (Strömberg and Banwart, 1999a) and dynamic (Strömberg and Banwart, 1999b) laboratory tests of rock weathering, tracer studies of solute transport in the field and in laboratory reactors (Eriksson et al., 1997) and analysis of spatial variability in site properties to resolve apparent differences in reactive transport behaviour in the lab and in the field (Malmström et al., 2000a).

Being aware of the fact that lack of site data is a general obstacle to assessing mine water pollution in practice, we have developed a simple conceptual framework for preliminary assessment of minewater pollution corresponding to initial site assessment for Tier 1 decisions. The model can be used to estimate contamination source strength and longevity as well

Table 1
The stoichiometry of some weathering- and oxidation reactions

	Process	Reaction stoichiometry	Tracer
a	Pyrite oxidation (oxygen path)	$FeS_2(s) + H_2O + 7/2O_2(aq) \rightarrow Fe^{2+} + 2SO_4^{2-} + 2H^+$	Fe, SO_4^{2-}
b	Ferrous iron oxidation	$2Fe^{2+} + 1/2O_2 + 2H^+ \rightarrow 2Fe^{3+} + H_2O$	Fe
c	Ferric iron precipitation	$Fe^{3+} + 3H_2O \rightleftharpoons Fe(OH)_3(s) + 3H^+$	Fe
d	Pyrite oxidation by (ferric iron path)	$14Fe^{3+} + FeS_2(s) + 8H_2O \rightarrow 2SO_4^{2-} + 15Fe^{2+} + 16H^+$	Fe, SO_4^{2-}
e	Sphalerite oxidation	$ZnS(s) + 2O_2(aq) \rightarrow Zn^{2+} + SO_4^{2-}$	Zn^{2+}, SO_4^{2-}
f	Chalcopyrite oxidation	$CuFeS_2(s) + 4O_2(aq) \rightarrow Fe^{2+} + Cu^{2+} + 2SO_4^{2-}$	Fe, Cu^{2+} SO_4^{2-}
g	Calcite weathering $6 \leq pH \leq 9$	$CaCO_3(s) + H^+ \rightarrow Ca^{2+} + HCO_3^-$	Ca^{2+}
h	Calcite weathering $pH \leq 6$	$CaCO_3(s) + 2H^+ \rightarrow Ca^{2+} + CO_2(g) + H_2O$	Ca^{2+} (CO_2(g))
i	Dolomite weathering $6 \leq pH \leq 9$	$MgCa(CO_3)_2(s) + 2H^+ \rightarrow Mg^{2+} + Ca^{2+} + 2HCO_3^-$	Mg^{2+}, Ca^{2+}
j	Dolomite weathering $pH \leq 6$	$MgCa(CO_3)_2(s) + 4H^+ \rightarrow Mg^{2+} + Ca^{2+} + 2CO_2(g) + 2H_2O$	Mg^{2+}, Ca^{2+} (CO_2(g))
k	Biotite weathering	$K(Mg,Fe)_3AlSi_3O_{10}(OH)_2(s) + 7H^+ \rightarrow K^+ + 3(Mg^{2+}, Fe^{2+}) + Al(OH)_3(s) + 3SiO_2(s) + 3H_2O$	K^+, Fe, Mg^{2+}
l	Plagioclase weathering (oligoclase)	$Na_{0.7}Ca_{0.3}Al_{1.3}Si_{2.7}O_8(s) + 1.3H^+ + 1.3H_2O \rightarrow 0.3Ca^{2+} + 0.7Na^+ + 1.3Al(OH)_3(s) + 2.7SiO_2(s)$	Ca^{2+}, Na^+

as possible future changes in discharge quality. In the model, which represents a simple mass balance approach, the current contamination source strength is estimated from discharge quantities and qualities at the site. The acidity-producing and neutralising capacities of the material are calculated from bulk mineralogical or solid phase chemical composition, as shown below. The prediction of a potential onset of acidic drainage production is based on the known relative reactivity of different minerals and the estimated lifetimes of these minerals. The model is to be seen as a preliminary approach that may help screen sites and provide a basis for prioritising further site specific investigations between different sites and site objects. Further site studies may potentially include additional field and laboratory investigations as well as more detailed modelling. To illustrate the suggested approach, we assess three sites for which (limited) data have been reported in the literature: a mine rock waste deposit located above the water table, a flooded abandoned coal mine with deep workings and a mine tailings deposit. The preliminary assessment presented for these sites was carried out as a desk study using generally available information on discharge quantities and quality and site information from mine records. We conclude that even such simple hydrochemical mass balance models of a site are essential as a first step in understanding potential risk from a site.

1.1. Minewater hydrochemistry

Table 1 lists some important reactions that control the hydrochemical composition of mine water drainage. Pyrite weathering releases soluble ferrous iron (Fe^{2+}) and acidity which is represented by production of protons (Table 1, Reaction (a)). If sufficient dissolved oxygen is present, or if solutions can be oxygenated by contact with the atmosphere, the dissolved ferrous iron will be oxidised to ferric iron (Fe^{3+}), consuming acidity in the process (Reaction (b)).

A much greater net production of acidity occurs because ferric iron can react further to precipitate as iron oxyhydroxide mineral (Reaction (c)), or by reacting further with the pyrite to produce more acidity and ferrous iron (Reaction (d)). Because the forward and reverse reactions are relatively rapid for the precipitation and dissolution of ferric hydroxide, compared to residence times of discharge water in mine workings, minewaters often achieve solubility equilibrium with these minerals. This is denoted by writing Reaction (c) in Table 1 as both a forward and reverse reaction at equilibrium.

The ferrous iron produced in Reaction (d) can then be re-oxidised by available dissolved oxygen, perpetuating the cycle represented by Reactions (b)–(d). If dissolved oxygen becomes depleted, Reaction (d) can proceed to completion yielding predominantly ferrous iron in solution. Metal sulphides other than pyrite will

not necessarily produce acidity, but will release soluble metal ions to solution. Examples are given in Table 1 as the oxidation of sphalerite (Reaction (e)) and of chalcopyrite (Reaction (f)), which release zinc and copper ions, respectively, to solution.

It is clear from these weathering reactions that water infiltrating a mine site will accumulate solutes as minerals dissolve along the water pathway. As acidity is released to solution during pyrite weathering, the pH will drop. There are other minerals however, that can consume acidity as they dissolve, thereby providing natural attenuation of the acidity produced by pyrite weathering, helping to buffer the pH. This is a critical aspect of assessing minewater contamination since the solubility and therefore the mobility and bioavailability of metal ions is strongly pH dependent. Below neutral pH, metal ions generally have increasing solubility with decreasing pH. Natural attenuation of acidity and pH buffering turn out to be critical controls on the environmental behaviour of metal ions that are released in minewater discharges.

The weathering of many carbonate and silicate minerals consumes acidity and helps buffer pH. We apply a rigorous definition of acidity and alkalinity as "the amount of strong base or strong acid that must added to raise (acidic conditions) or lower (alkaline conditions) the pH to a reference value that corresponds to the carbonic acid equivalence-point in the open H_2O–CO_2-system". In a system at standard conditions (25°C, 1 atm) this pH is 5.6 if atmospheric partial pressure of carbon dioxide gas is maintained at equilibrium with pure water. The equivalence-point pH is lower if the water is prevented from exchange with the gas phase as sometimes assumed for titrations (around pH 4.5 and dependent on the total acidity/alkalinity) or is in equilibrium with higher partial pressures of carbon dioxide as may be the case if, for example, extensive carbonate mineral weathering has occurred. A minewater discharge contains alkalinity if the equilibrium (with the receiving water) pH is above the reference pH, and contains acidity if the equilibrium pH is below this value.

There are also a number of laboratory tests that provide an operational assessment of the available acid neutralising and acid producing capacity of mine waste and ore rock. The US EPA have published a standard method of Acid Base Accounting (ABA, Sobek et al., 1978). The method compares the acid-neutralising capacity, termed 'neutralisation potential' (NP), with the base-neutralising capacity, or 'acidity potential' (AP), in order to determine if a particular material is expected to produce acidic effluents at a mine site. The NP is determined by reacting a known mass of crushed rock with a known excess of concentrated hydrochloric acid while heating for a fixed period of time. The residual acidity after reaction is determined by titrating the supernatant acid. The AP is determined by chemical analysis of the rock, relating total sulphur content to equivalents of sulphuric acid (H_2SO_4) that could be formed from sulphide mineral weathering. The 'net neutralisation potential' (NNP) is the difference between the two values reported in the equivalent mass of calcium carbonate (g $CaCO_3$(s) per Kg rock).

A number of shortcomings and subsequent modifications to the procedure have been presented (Li, 1997; Kwong and Ferguson, 1997; Lawrence and Wang, 1997). For example, it is known that reacting samples with concentrated hydrochloric acid at high temperature may overestimate NP since rock will be less reactive under field conditions (Paktunc, 1999b). Mineralogical information is also needed when interpreting NP since neutralising capacity can originate from a variety of minerals that react at very different rates under field conditions (Paktunc, 1999a,b).

Additional assays have been developed, including measurement of 'net acid generation' (NAG) where rock is reacted with hydrogen peroxide at room temperature until available sulphide mineral is exhausted by chemical oxidation (Finkelman and Giffin, 1986; O'Shay et al., 1990). Humidity cell experiments can be carried out on uncrushed mine rock to assess if and when the rock will become acid-producing (ASTM, 1996; Price, 1997). A typical procedure is to subject rock samples to dry air flow for several days, followed by an equal period of exposure to water-saturated air and finally followed by flushing with water to mobilise accumulated solutes from the material. The cycle is then repeated for a period of weeks up to a year. Onset of acid production is noted by a corresponding drop in pH. Kinetic tests also include laboratory column reactors where rock is reacted with water flow through the columns. Rates of solute production are determined by analysing water flow rates and solute concentrations in the effluent.

All of these tests aim to use observations under controlled reaction conditions that can then be extrapolated to field conditions. However, the very large differences in the physical scale and complexity between laboratory tests and field sites makes such extrapolation very uncertain. There is recent evidence that, in some cases, such extrapolation may be made reliably if a number of physical and chemical characteristics of a mine site are quantified (Malmström et al., 2000a). These include particle size distribution for the rock at a site, variations in mineralogy with particle size fraction, temperature and pH effects on weathering rates, spatial variation of mineralogy within a site, preferential subsurface water flow and the availability of O_2 in the subsurface.

In the absence of data on NNP, NAG, weathering rates and detailed site data such as the physical-chemical factors listed above, an additional method of assessing reaction rates at field scale is to use solute flows in the site discharge as tracers for the reactions that produce and consume acidity. The basic data required are water flows from the site, and the solute concentrations in these flows. This represents a kinetic test at field scale, and is appropriate for preliminary assessment of contaminant loads and their evolution with time, as part of a Tier 1 decision making processing as described above. In most instances, there is a lack of detailed site-specific information on factors that limit the availability of carbonate minerals and sulphides to consume and produce acidity through weathering reactions at a field site. In this case, upper limits to these chemical capacities are estimated by the total amounts of the respective minerals present.

The purely theoretical definition for acidity and alkalinity given above is very useful in practical terms. The acidic range of the carbonic acid equivalence-point ($pH < 5.6$) broadly corresponds to conditions where mineral oxide and hydroxide precipitates that immobilise metal ions are relatively more soluble. Conversely, the alkaline range ($pH > 5.6$) corresponds to conditions where such mineral phases are generally much less soluble, thus immobilising metal ions. Two very broad categories of environmental risk are thus defined for minewater pollution, in terms of acidity and alkalinity and the associated ranges in pH.

1. Acidic waters represent significant risk from soluble metals ions via water flow paths to sensitive receptors such as drinking water wells or receiving streams.
2. Alkaline waters represent significant reduction in such risk due to immobilisation of metal ions within the transport pathway.

Dissolution of calcite is a classical example of a weathering process that consumes acidity. This is represented in Table 1 by the Reactions (g) and (h) which consume protons and release calcium and bicarbonate ions and carbon dioxide to solution. It is clear that the rate of mineral weathering must be considered. If the rate of acid generation is faster than calcite weathering rates, then a discharge will be acidic no matter how large the available reservoir or calcite may be. Calcite generally dissolves sufficiently rapidly to maintain a minewater discharge in solubility equilibrium with the mineral if it is present. Although there is a range of carbonate minerals which can contribute to acid neutralisation (Paktunc, 1999b), we focus here on calcite for the sake of simplicity in developing the proposed model. In addition to calcite (and other carbonate minerals) dissolution, weathering of aluminosilicate minerals, represented by mica (biotite) and feldspar (anorthite, albite and K-feldspar) in Reactions (k) and (l) in Table 1, consumes acidity, although rates of dissolution are much slower than for calcite. These aluminosilicate oxides provide acid-neutralising capacity through release of oxide ions (O^{2-}) from the crystal lattice to solution. These ions are strong bases and become protonated below pH 14 to form OH^- and H_2O. Aluminium that is released during weathering of these minerals acts as a weak acid that releases protons through hydrolysis reactions. The free ion Al^{3+} remains the dominant dissolved species when weathering takes place below pH 4, but can release acidity due to hydrolysis when weathering takes place at higher pH conditions. The net effect of aluminosilicate weathering is thus to provide acid-neutralising capacity through slow weathering reactions. However, the equivalents of acid that are neutralised by each mole of mineral that dissolves, is smaller at progressively higher pH conditions due to Al^{3+} hydrolysis.

Fig. 1 compares laboratory weathering rates for pyrite with those for some carbonates and silicates. Calcite dissolves approximately 3 orders-of-magnitude

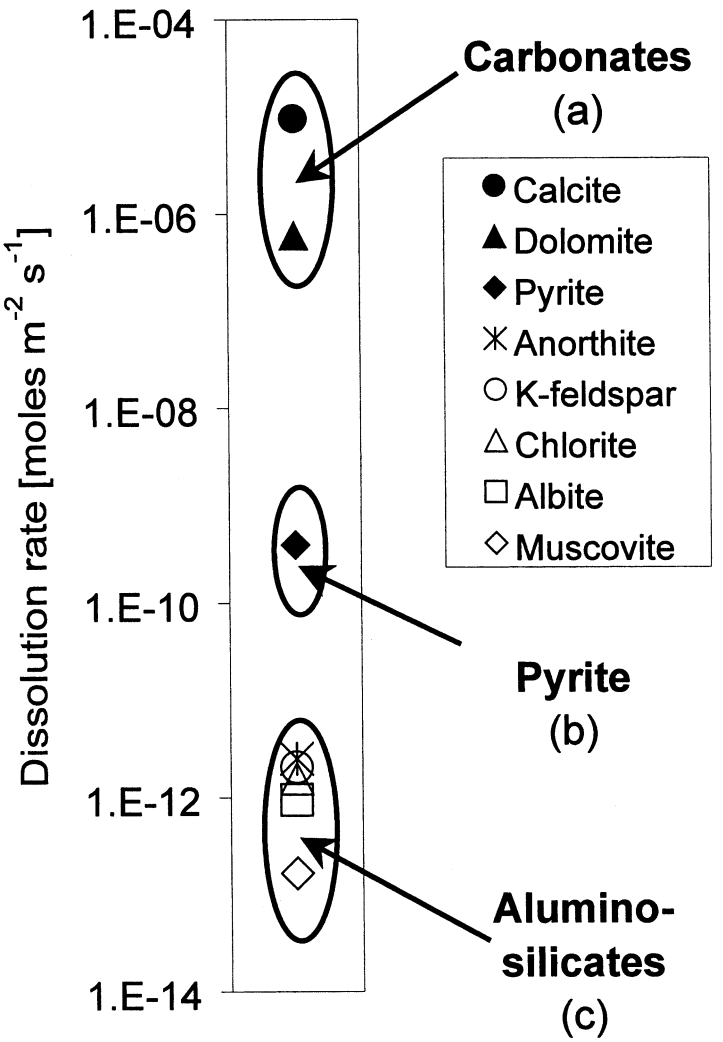

Fig. 1. Surface area normalised dissolution rates for source minerals far from solubility equilibrium at oxic conditions and pH 5 and 25°C (mol m^{-2} s^{-1}) (a) calcite and dolomite (data from Chou et al. (1989), and Gautelier et al. (1999), respectively); (b) pyrite (data from Williamson and Rimstidt (1994)); (c) aluminosilicates (data from compilation in White and Brantley (1995), and Sverdrup (1990)).

more quickly than pyrite, which in turn dissolves nearly 3 orders-of-magnitude more quickly than the aluminosilicates. These relative rates of dissolution suggest that if the minerals are available in similar quantities, calcite weathering will produce alkalinity at a rate that is sufficient to neutralise the acidity produced from pyrite weathering and maintain pH at circumneutral values. On the other hand, if calcite is effectively depleted, then acidic discharges are expected. Note also that in the absence of other buffering minerals, silicate weathering will provide alkalinity, albeit at a lower rate than calcite. The actual level of acidity will in this case be determined by the relative rates of pyrite and silicate weathering.

In addition to providing a simple prediction of whether a discharge will be acidic or alkaline, this concept can be extended to changes in discharge water quality over time. Fig. 2 shows the conceptual development of minewater discharge pH due to depletion of first calcite and subsequently pyrite, which occur at the lifetime of the mineral.

Because metal ion mobility is linked so strongly to

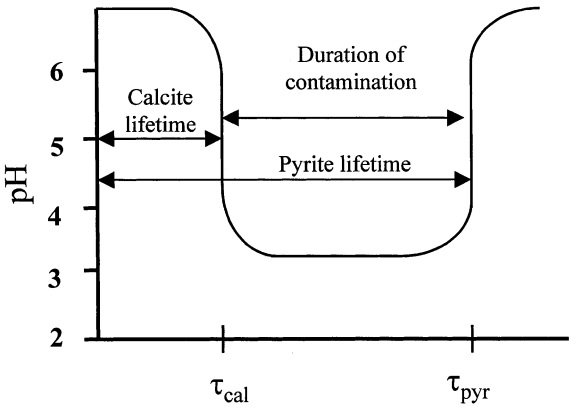

Fig. 2. Schematic diagram showing the relationship between trends in pH with the lifetime of minerals that produce and consume acidity.

acidic conditions, depletion of pyrite and cessation of acidity production provides a critical time scale corresponding to the severest contamination release from a mine site. In broad terms, the lifetime of pyrite, τ_{pyr}, corresponds to the contaminating lifetime of the site, but that discharge may remain near-neutral throughout this period of time if the lifetime of calcite, τ_{cal}, is large enough ($\tau_{pyr} < \tau_{cal}$). This model for evolution of minewater discharge quality is summarised as follows:

- If $\tau_{cal} < \tau_{pyr}$, the discharge will become acidic at time τ_{cal};
- If $\tau_{pyr} < \tau_{cal}$, the discharge will remain alkaline;
- τ_{pyr} defines the contaminating lifetime for the highest metal contamination loads.

Fig. 3 shows the dynamic behaviour of pH and metal ion mobility that occurs due to calcite depletion.

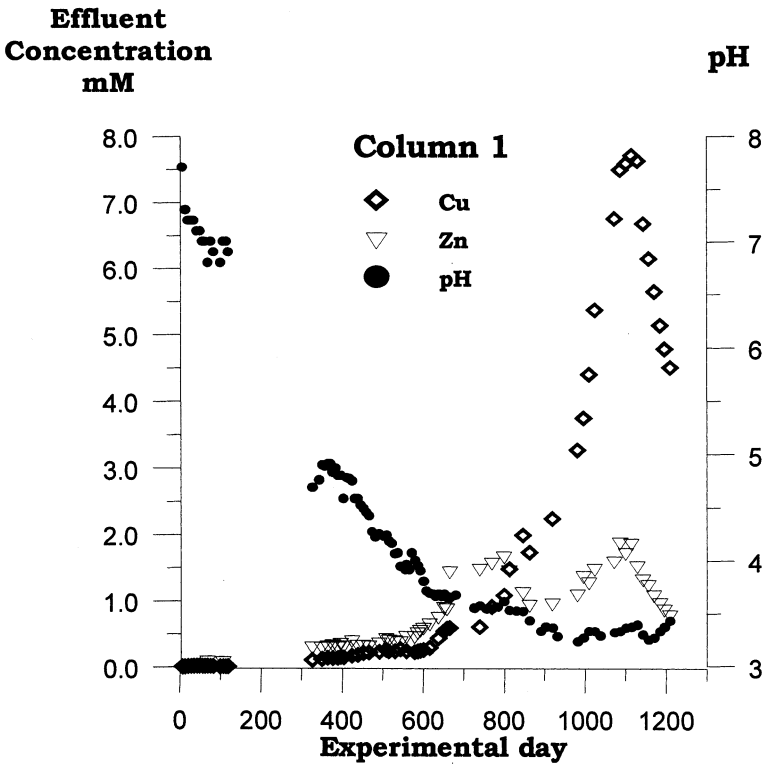

Fig. 3. Results from a column reactor showing the impact of calcite depletion on pH and mobility of copper and zinc ions (data from Strömberg and Banwart (1999b)). The waste rock in the reactor contains little calcite which becomes depleted (around day 900), resulting in a subsequent drop in pH, and a corresponding mobilisation of zinc and copper ions. When all the attenuated zinc and copper has been flushed, the release rates decrease to levels corresponding to the metal sulphide weathering rates (see Strömberg and Banwart (1999b) for a detailed discussion).

Table 2
Equations for calculating the solute flow, the mineral weathering rate, the mineral content, and the mineral lifetime using hydrochemical tracers (F_W is the water flow (l s^{-1}) and F_c and F_c^m are the flow of the contaminant in units of (mol s^{-1}) and (mg s^{-1}), respectively. C_c and C_c^m are the concentration of the contaminant in units of (mol l^{-1}) and (mg l^{-1}), respectively. N_t and N_M (mol) are the amount of the tracer t and the mineral M, respectively. A is the areal extent (m^2) and H is the height (depth) (m) of the deposit. m_{TOT} (kg) is the mass of the rock, m_M is the mass of mineral M (g) and m_t is the mass of tracer t (g). V_{TOT} is the volume of the deposit (m^3) and V_M is the volume of mineral M (m^3). $R_{w,M}$ is the mineral weathering rate (mol s^{-1}) and τ_M is the mineral lifetime (s). γ_M is the volume fraction of mineral M (m^3 m^{-3}) and ν_{wm} is the porosity of the deposit (m^3 m^{-3}). δ_{wm} and $\delta_{wm,c}$ are the density and the compact density of the deposit (kg m^{-3}), related through $\delta_{wm} = \delta_{wm,c}(1 - \nu_{wm})$, and δ_M is the density of mineral M (kg m^{-3}). $M_{w,M}$ and $M_{w,t}$ are the molecular weights (g mol^{-1}) of mineral M and of tracer t, x_t is the mass fraction of tracer t (g g^{-1}), and $n_{t,M}$ is the stoichiometric coefficient of tracer t in mineral M, whereas $\eta_{t,M}$ is the stoichiometric coefficient of tracer t in the weathering reaction for mineral M)

Solute flows	Volume
$F_c = \sum_i F_{W,i}C_{c,i} - \sum_j F_{W,j}C_{c,j}$ mol s^{-1}	$V_{TOT} = AH$ m^3
$F_c^m = \sum_i F_{W,i}C_{c,i}^m - \sum_j F_{W,j}C_{c,j}^m$ mg s^{-1}	$V_M = AH\gamma_M(1 - \nu)$ m^3
$F_c = \frac{F_c^m 10^3}{M_{w,t}}$ mol s^{-1}	Mass
Weathering rate	$m_{TOT} = V_{TOT}\delta_{wm}$ kg
$R_{w,M} = \frac{F_{t,M}}{\eta_{t,M}}$ mol s^{-1}	$m_M = N_M M_{w,M}$ g
Moles	$m_M = V_M\delta_M$ kg
$N_t = \frac{m_t 10^3}{M_{w,t}}$ mol	$m_t = m_{TOT}x_t$ kg
$N_M = \frac{N_t}{n_{t,m}}$ mol	Mineral lifetime
$N_M = \frac{m_M 10^3}{M_{w,M}}$ mol	$\tau_M = \frac{N_M}{R_{w,M}}$ s

As expected, depletion of calcite corresponds to a significant drop in pH (around day 900; see Strömberg and Banwart (1999b) for details). Metal ions that had been previously immobilised at neutral pH are mobilised and flushed with the effluent as pH drops. When the metal ions that have been attenuated in secondary phases and/or sorbed during the period of weathering at circumneutral pH have been flushed, the metal release rates decrease to levels that correspond to the metal sulphide weathering rates. This behaviour illustrates the importance of anticipating whether minewater discharge quality will deteriorate as existing natural attenuation capacity is depleted. If deterioration is expected, the timing of the pH drop is critical since it is expected to coincide with a potentially serious, elevated loading of metals contamination.

The relative rates of mineral weathering for calcite, pyrite and aluminosilicates provides the basis for this conceptual model of the evolution of minewater discharge quality over time. Critical parameters that need to be assessed are the time to depletion for pyrite and calcite. These values can be estimated from solute flows in a discharge, and estimates of the mineral mass within the mine site. For example, sulphate ions in the discharge provide a natural tracer for oxidation of sulphide, while base cations and metal ions provide tracers for dissolution of their respective source minerals. If these tracers are conserved during dissolution and transport with flow from the site, then knowledge of solute concentrations and discharge rates yields the solute flows and provides an estimate of the mineral weathering rates at the site.

2. Using hydrochemical tracers to assess mine water pollution

In order to estimate the current mineral weathering rates at a site, we need to make an integrated solute mass-balance. Such a mass-balance is based on the water budget, including surface and groundwater flows, and the associated water qualities and also yields the present contaminant load from the site (source strength). The approach is conceptually the same when considering underground workings or waste rock or tailings deposits above ground. Eq. (1) shows how the flow, F_c, of a contaminant due to processes in a rock or ore deposit is obtained from the various water flows, F_W, and the contaminant concentrations, C_c (Table 2) at steady-state conditions.

$$F_c = \sum_i F_{W,i}C_{c,i} - \sum_j F_{W,j}C_{c,j} \qquad (\text{mol s}^{-1}) \qquad (1)$$

In Eq. (1), i and j denote flows from and to the deposit, respectively.

If the water residence time is short in comparison to the time-scale of other processes in the deposit, e.g. the depletion of minerals, and no accumulation of solutes occur within the deposit, then the determined solute flow reflects the rate of ongoing biogeochemical processes. Hence, if we can assign the flow of a solute to be mainly the effect of a certain process with known stoichiometry, we can estimate the rate of that process.

Inspection of Table 1 shows that mineral weathering reactions release a variety of solutes that can be used as hydrochemical tracers for the weathering processes. The term 'tracers' within this context, is used to denote that these solutes are reaction products that trace, i.e. provide direct evidence of, specific weathering reactions whose rates can be quantified through hydrochemical assessment. Eq. (2) shows how a flow of a tracer, $F_{t,M}$, is related to the rate of the associated weathering process, $R_{w,M}$

$$R_{w,M} = \frac{F_{t,M}}{\eta_{t,M}} \qquad (\text{mol s}^{-1}) \tag{2}$$

where $\eta_{t,M}$ is the stoichiometric coefficient for tracer t in the weathering reaction of mineral M.

Having obtained the current weathering rate, an estimate of the duration of the weathering reaction is obtained by calculating the lifetime of the mineral in the deposit. As a first approximation, the current rate of weathering is assumed to remain constant until the entire content of the mineral in the deposit has been consumed. For this case, the lifetime, τ_M, of a mineral is related to the molar amount of the mineral in the deposit, N_M, and the weathering rate as

$$\tau_M = \frac{N_M}{R_{w,M}} \qquad (\text{s}) \tag{3}$$

More accurate estimates of the mineral lifetime and of the time evolution of the contaminant flow rely on a relevant conceptual model for the time-dependence of the weathering rate and must assess the rate-limiting step in the process. Standard kinetic rate expressions for detailed chemical reaction modelling are based on the 'shrinking core model' (Evans, 1979) that accounts for intraparticle O_2 mass transfer limitation, or the 'shrinking particle model' (Scharer et al., 1994) that accounts solely for surface reaction limitation on weathering rates.

The amount of mineral, the 'mineral budget', is determined by the areal extent and depth (height) of the source as well as on the composition of the rock and ore in it. Eqs. (4a) and (4b) show how the mineralogical composition as vol.% of minerals, determined from e.g. thin sections and the chemical composition reported in terms of mass% of elements, determined e.g. from chemical analyses, are related to the molar amount of the mineral in the deposit (Table 2)

$$N_M = \frac{AH\gamma_M\delta_{wm}}{M_{w,M}} \qquad (\text{mol}) \tag{4a}$$

$$N_M = \frac{AH\delta_{wm}x_t}{n_{t,M}M_{w,t}} \qquad (\text{mol}) \tag{4b}$$

In Eqs. (4a) and (4b), A is the areal extent of the deposit, H is the height (depth) of the deposit, γ_M is the volume fraction of mineral M, δ_{wm} is the density of the rock or ore, $M_{w,M}$ and $M_{w,t}$ are the molecular weight of mineral M and of tracer t, x_t is the mass fraction of tracer t, and $n_{t,M}$ is the stoichiometric coefficient of tracer t in mineral M. The density of the material can be obtained from the compact density, $\delta_{wm,c}$, and the porosity, ν_{wm}, *as:* $\delta_{wm}(1 - \nu_{wm})\delta_{wm,c}$.

3. Three case studies

3.1. The Aitik site

3.1.1. Site description

The Aitik mine, located close to Gällivare in the northern part of Sweden, is Europe's largest operating copper mine, producing also waste rock that is deposited in heaps at the site. The Aitik waste rock heaps currently extend over an area of about 260 ha with a depth of 15–20 m and have been well characterised in terms of physicochemical parameters, mineralogy, chemistry and hydrology (Strömberg and Banwart, 1994, 1999a,b; Eriksson et al., 1997). The owner, Boliden Mineral AB, has applied dry covers on the heaps following the outcome of a programme for assessing protective measures after mining activities. This case study assesses the situation prior to remediation at which point the heaps were unsaturated with respect to water, with an average water content of about 10 vol.%. The heaps, which contain rock material with fragments up to the order of 1 m

Table 3
Physical, mineralogical and chemical characteristics of the waste rock heaps and associated drainage water at the Aitik site (data as summarised by Strömberg and Banwart (1994))

Physical data		Hydrological data		Mineralogical composition of waste rock		Drainage water quality[a]		
					Vol.%		West ditch	East ditch
Areal extent[b]	2.6×10^6 m^2							
Height (average)	20 m	Precipitation	680 mm year^{-1}	Quartz	24 ± 14		D1	D2
Temperature annual average at site	0°C	Water flow rate		K-feldspar	24 ± 19	pH	3.8 ± 0.1	4.2 ± 0.4
Estimated average in heap	5°C	West ditch (D1)	10 m^3 min^{-1}	Plagioclase	19 ± 14	SO_4^{2-}	1310 ± 250	220 ± 97
Porosity	0.35	East ditch (D2)	2 m^3 min^{-1}	Muscovite	10 ± 16	Fe_{Tot}	2.0 ± 1.0	2.8 ± 1.9
Rock density[c]	2800 kg m^{-3}	Water residence time	1.5 years	Biotite	8 ± 7	Cu^{2+}	19 ± 5.0	1.2 ± 0.8
Specific surface area of waste rock	1.0 m^2 g^{-1}			Skarn and accessory minerals	11 ± 25	Zn^{2+}	5.8 ± 1.6	0.4 ± 0.3
				Calcite	0.1 ± 0.5	Ca^{2+}	185 ± 46	47 ± 24
				Pyrite	0.57	Mg^{2+}	57 ± 13	11 ± 5.7
				Chalcopyrite	0.09			

[a] mg l^{-1} except for pH.
[b] Correction of the 4.00×10^6 m^2 reported by Strömberg and Banwart (1994).
[c] In the calculations, representative compact mineral densities of sulphide and silicate minerals of 5100 and 2700 kg m^{-3}, respectively, were used.

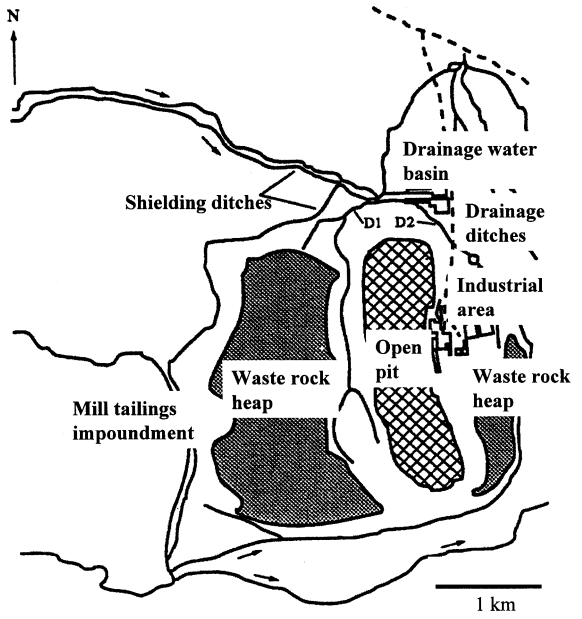

Fig. 4. Map of the Aitik site showing the waste rock heaps surrounding the open pit (from Strömberg and Banwart (1994)).

diameter, remain predominantly oxic over their full depth, with measured oxygen concentrations in the pore gas ranging from 3 to 21 vol.%. The surface temperature at the site varies considerably, with average winter and summer temperatures of −15 and 15°C, respectively, whereas the temperature in the major part of the heaps was fairly constant around 4°C. The drainage water from the heaps, which is collected in two ditches and used as process water in the enrichment plant, has a pH of 3.8–4.2 (Table 3). The low pH in the drainage water indicates that available carbonates (mainly calcite) have been depleted to a large degree.

3.1.2. Site assessment

The dominant acidity producing processes in the Aitik waste rock heaps have been identified to be oxidative weathering of pyrite and subsequent precipitation of ferric oxyhydroxide (Strömberg and Banwart, 1994; Reactions a and c in Table 1):

$$FeS_{2(s)} + 15/4O_{2(aq)} + 7/2H_2O \rightarrow Fe(OH)_{3(s)} + 2SO_4^{2-} + 4H^+ \quad (5)$$

The dominant reaction for copper mobilisation at the Aitik site has been identified to be oxidative weathering of chalcopyrite (Strömberg and Banwart, 1994; Reaction f in Table 1). The low pH of the drainage water indicated that available calcite has been depleted, or is no longer reacting sufficiently rapidly to release significant amounts of Ca^{2+} as has been demonstrated for larger rock particles at the site (Strömberg and Banwart, 1999a). Hence, we consider plagioclase as the source of Ca^{2+}. The weathering of biotite, $K(Fe_{1.5}Mg_{1.5})(AlSi_3O_{10})(OH)_2$ (Compare Reaction k), and weathering of plagioclase (with a composition of 30% anorthite, $CaAl_2Si_2O_8$, and 70% albite, $NaAlSi_3O_8$; Reaction l in Table 1) then remain as the major acidity consuming processes. The weathering of, e.g. muscovite and K-feldspar, which also are dominant silicates in the Aitik waste rock, is much slower and contributes less to the proton consumption at the site (Strömberg and Banwart, 1994).

To estimate the solute flows from the site, average concentrations of solutes were multiplied by average flow rates in the ditches draining the waste rock heap (Tables 2 and 3). The total solute flows from the site were obtained by summing flows in ditches 1 and 2 (Fig. 4). Hydrological investigations and ground water monitoring indicate that only a small fraction of the water flow infiltrates the subsurface below the heaps (Axelsson et al., 1992). Therefore, solutes originating from weathering processes in the heaps are transported from the site via the ditches. Hence, solute flows in these ditches represent integrated weathering rates at the site.

Weathering rates for chalcopyrite, R_{chp}, and pyrite, R_{pyr}, were determined from the flow of Cu^{2+} and sulphate respectively. The sulphate arising from chalcopyrite weathering was accounted for using the mineral stoichiometry. The equivalent flow of sulphate was subtracted from the total in order to obtain the pyrite weathering rate:

$$R_{chp} = F_{Cu^{2+}} \ (\text{mol s}^{-1}) \quad (6)$$

$$R_{pyr}^{SO_4^{2-}} = \frac{(F_{SO_4^{2-}} - 2R_{chp})}{2} = \frac{(F_{SO_4^{2-}} - 2F_{Cu^{2+}})}{2} \ (\text{mol s}^{-1}) \quad (7)$$

Silicate weathering rates were calculated from Ca^{2+} and Mg^{2+} flows assuming that Ca^{2+} originates

Table 4
Estimated solute flows, mineral weathering rates, mineral contents and mineral lifetimes for the waste rock heap at the Aitik site

Solute flows			Mineral contents			Mineral weathering rates		Mineral lifetimes	
	Mol s^{-1}	Tonnes $year^{-1}$		Mol	kg		Mol s^{-1}		Years
SO_4^{2-}	2.4	7116	Pyrite	8.2×10^9	9.8×10^8	Pyrite	1.1	Pyrite	231
Cu^{2+}	5.0×10^{-2}	101	Chalcopyrite	8.5×10^8	1.6×10^8	Chalcopyrite	5.0×10^{-2}	Chalcopyrite	530
Ca^{2+}	0.81	1022	Plagioclase	6.7×10^{10}	1.7×10^{10}	Plagioclase	2.7	Plagioclase	791
Mg^2	0.41	311	Biotite	2.1×10^{10}	9.7×10^9	Biotite	0.27	Biotite	2455

from plagioclase and Mg^{2+} from biotite. Hence, when accounting for the mineral stoichiometries (Table 1), we obtained the weathering rates of biotite, R_{Bio}, and plagioclase, R_{Pla}, from

$$R_{Bio} = \frac{F_{Mg^{2+}}}{1.5} \quad (\text{mol s}^{-1}) \tag{8}$$

$$R_{pla} = \frac{F_{Ca^{2+}}}{0.3} \quad (\text{mol s}^{-1}) \tag{9}$$

Mineral abundance was quantitatively characterised from drill cores by thin-section and mineral chemical analysis. From reported areal extent and height of the heap, porosity and volume fractions of the minerals (Table 3), we calculated the volume of the individual minerals in the deposit. These volumes were converted to the molar amounts for each mineral using the respective mineral densities and molecular weights (Table 2). Mineral life times were obtained by dividing moles of each mineral by the respective weathering rate (Eq. (3)).

3.1.3. Results and implications

Table 4 lists the solute flows, mineral weathering rates, mineral content and mineral lifetimes. A detailed geochemical model has already been used to assess mineral lifetimes at the site (Strömberg and Banwart, 1994). Results from our model show lifetimes that are approximately a factor of two smaller than those in the previous investigation. The main discrepancy between the models arises from differences in the areal extent of the deposit which was overestimated by a factor of 1.5 in the previous assessment.

Pyrite and chalcopyrite are predicted to occur over time scales of centuries. This implies that passive remediation methods are required for site restoration. The site owners have covered the site to reduce oxygen ingress and acid mine drainage (AMD) generation.

The presence of calcite in the freshly deposited waste (Table 3) is expected to initially maintain circum neutral pH and calcite solubility equilibrium with pore waters. As indicated by the relative amounts of calcite and pyrite and the reported, associated acid producing ($\sim$700 meq. kg^{-1}) and neutralising ($\sim$100 meq. kg^{-1}) capacities of the material (Strömberg, 1997), depletion of calcite prior to pyrite is expected. Because equilibrium between the aqueous phase and calcite is not observed, we conclude that calcite either already has been fully depleted or is distributed within the rock mass such that its weathering does not interact with drainage water. The depletion of calcite disseminated within waste rock has been previously experimentally demonstrated and modelled (Strömberg and Banwart, 1999a). Assuming that calcium originates from plagioclase dissolution, the lifetimes of this mineral and other silicates is on the order of millennia. This suggests that these reactions will contribute alkalinity throughout the period of sulphide weathering. The actual degree of neutralisation of the acidity released during sulphide weathering is determined by the relative rates of sulphide and silicate mineral weathering rates. These rates are dependent on factors such as oxygen- and mineral availability and are expected to vary over time.

The Aitik site has been the subject of an extensive research investigation into transport and reaction processes that control AMD loads (see summaries by Eriksson (1996) and Strömberg (1997)). An important conclusion was that only a fraction of the water mass is mobile (65%; Eriksson et al., 1997) within the heap and thus contributes to the solute flows. If the

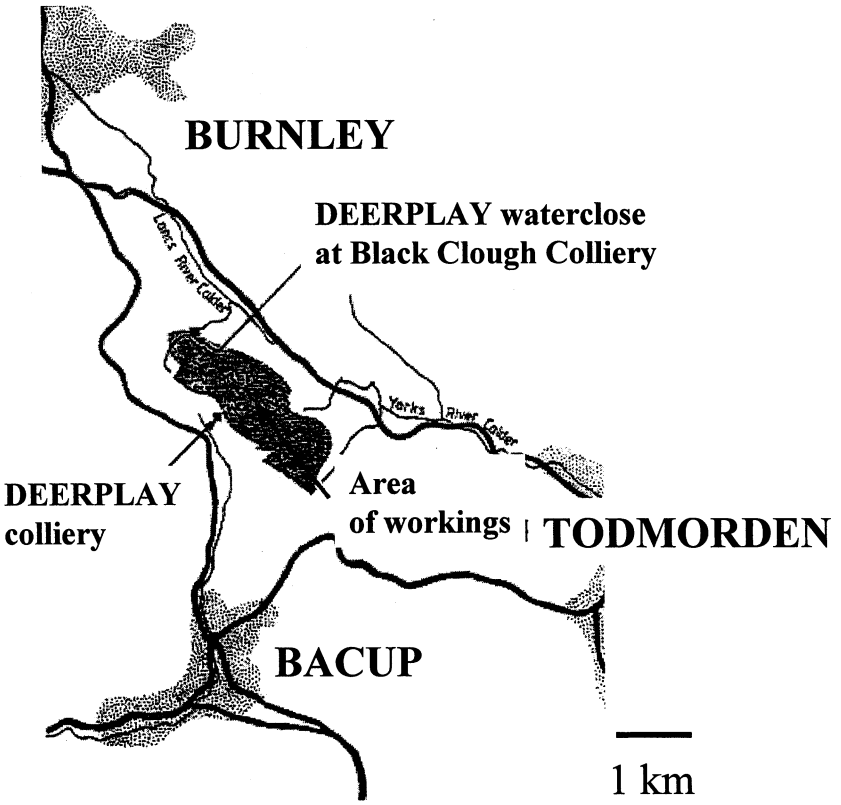

Fig. 5. Map of the Black Clough site showing the location of the Deerplay Waterloose which drains the mine, and the extent of the underground workings drawn as the shaded area between the Deerplay Colliery and the Deerplay Waterloose (from the Environment Agency of England and Wales).

rock mass that generates AMD at the site is reduced to include only the part that is actually drained this would result in correspondingly lower lifetimes of the minerals with respect to generation of AMD. The site assessment presented here results in a conservative estimate of contaminant duration since calculated mineral lifetimes correspond to upper limits.

3.2. The Black Clough site

3.2.1. Site description

The Black Clough stream descends from Deerplay Moore in the Penine Hills of northern England, approximately 5 km to the southeast of Burnley, Lancashire. Fig. 5 shows the location of the mine-water discharge which resulted from the abandonment of a coal seam worked by three collieries, namely Deerplay, Black Clough and Hilltop. In 1968 the last of the three mines, Hilltop, was closed and dewatering by pumping ended. In May, 1969, six months after cessation of pumping, highly ochreous water was discharged from the Black Clough portal which had been left open for drainage when the mines were abandoned. Subsequent early discharges were highly contaminating with iron concentrations on the order of 450 mg l^{-1}. The abundance of carbonate minerals associated with the sedimentary strata surrounding the coal measures prevented the mine water from becoming acidic with current alkalinity values near 50 mg l^{-1} as $CaCO_3$(s) and dissolved iron concentrations near 60 mg l^{-1}. Although water quality has improved slowly during the ensuing decades, a steady release of ferruginous water has resulted in extensive iron oxide deposition and associated degradation of the stream bed and water quality for several kilometres downstream.

Table 5
Physical, mineralogical and chemical characteristics of the coal mine and groundwater at the Black Clough site (data as reported by Capewell (1996)) (na — not available)

Physical data		Hydrological data		Mineralogy of UK coal measure mudrocks		Groundwater quality		Chemical composition of Lower Mountain Coal Measures	
					Vol.%				
Areal extent	3.0×10^6 m^2	Precipitation	1344 mm year^{-1}			pH	6.5	Sulphur content (pyrite)	0.3 wt% S
Height (thickness of coal seam)	1.22 m	Runoff	1004 mm year^{-1}	Pyrite	2.5	SO_4^{2-}	460 (mg l^{-1})		
Temperature (annual average)	na	Water Discharge		Calcite	4.5	Fe_{Tot}	62 (mg l^{-1})		
Volume of coal removed	60%	Estimated	30.1 l s^{-1}			Ca^{2+}	127 (mg l^{-1})		
Porosity of collapsed working	0.4	Calculated	32.3 l s^{-1}						
Coal porosity	0.03	Water residence time	6 months						
Mudrock density[a]	2650 kg m^{-3}								
Coal density[a]	1260 kg m^{-3}								

[a] In the calculations, representative compact mineral densities of sulphide and silicate minerals of 5100 and 2700 kg m^{-3}, respectively, were used.

The abandonment plan states that for the main seam, the worked height is 1.22 m and the extent of the workings is estimated as 3 km^2 (Fig. 5.) Due to the age of the mining complex, it can be assumed that the area was mainly mined using the pillar and stall method. After closure, rising groundwater is likely to cause structural instability in both roof and pillars leading to roof collapse. Therefore it may be assumed that the mined voids of the former workings are infilled with predominantly mudstone which is the overlying strata in the Lancashire Coal Measures.

3.2.2. Site assessment

Discharge from the site has not been measured, but can be estimated from the areal extent of the underground workings and the annual average infiltration rate (precipitation minus runoff and evapotranspiration). Sulphate in the discharge arises solely from pyrite weathering and calcium arises from calcite dissolution. The solute flows were calculated from the estimated discharge rate and the ion concentrations. Based on the mineral stoichiometry the pyrite weathering rate, R_{pyr}, corresponds to one-half the sulphate flow (compare Table 1). Calcite weathering rate, R_{cal}, is directly obtained from the calcium flow

$$R_{pyr} = \frac{F_{SO_4^{2+}}}{2} \qquad (\text{mol s}^{-1}) \tag{10}$$

$$R_{cal} = F_{Ca^{2+}} \qquad (\text{mol s}^{-1}) \tag{11}$$

The values for mineral abundance in the coal and confining strata were taken from handbooks on mining geology that include information on the East Lancashire Coal Field where the site is located, and from mining records. Pyrite arises from that hosted in the coal, and also that within the mudrock strata confining the mined seam. The amount that is available for weathering is assumed to be all pyrite within the 'pillars' that remained after mining, and all pyrite within mudrock that is assumed to have collapsed into the workings. The volume of each material is based on 60% extraction, φ, of the coal within the mined seam, with mudrock collapsing into the mined void with a resulting porosity of 0.4 $m^3\ m^{-3}$. The bulk volume of unmined coal was first calculated from the areal extent of workings and the thickness of the coal seam. Taking into account the remaining coal volume, and the resulting volume of mudrock in the collapsed workings, the volume of coal and mudrock hosting reacting pyrite were calculated. Using the densities of the materials, the volumetric fraction of pyrite in the mudrock and the weight fraction of sulphur in the coal (Table 5), the mass of pyrite was subsequently calculated as the sum of the sulphur content of the coal, and the pyrite content in the mudrock, respectively

$$m_{pyr,coal} = HA\frac{(100-\varphi)}{100}\delta_{coal}\frac{x_S M_{v,pyr}}{M_{v,S}} \qquad (\text{kg}) \tag{12}$$

$$m_{pyr,mudstone} = HA\frac{\varphi}{100}(1-\nu)\gamma_{pyr}\delta_{pyr} \qquad (\text{kg}) \tag{13}$$

The calcite mass was calculated in the same way, but assuming that only the mudrock contains the mineral

$$m_{cal} = HA\frac{\varphi}{100}(1-\nu)\gamma_{cal}\delta_{cal} \qquad (\text{kg}) \tag{14}$$

The molar amount of each mineral was then calculated from these mineral masses and the corresponding molecular weights. The lifetime of each mineral was estimated by dividing the mineral mass by the weathering rate (Eq. (3)).

3.2.3. Results and implications

Table 6 lists the solute flows, mineral weathering rates, mineral content and mineral lifetimes. The duration of contamination is predicted to be on the order of centuries. The calculated mineral lifetimes for pyrite and calcite are similar. An important result is that the calcite lifetime is less than that of pyrite. The conceptual model for the evolution of minewater pH suggests that sites with a calcite lifetime that is less than that of pyrite, could potentially become acidic when calcite is depleted. Although the calculated lifetimes are only order-of-magnitude estimates, they indicate that this site could turn acidic at some point in the (possibly distant) future.

The enormous accumulation of iron oxyhydroxide that is resulting from the highly ferruginous discharge at Black Clough is expected to retain potentially toxic metal ions such as Cu^{2+}, Pb^{2+}, and Cd^{2+}. Such metals, typically originating as trace elements in sulphide phases present in sedimentary environments, sorb strongly on iron (hydr)oxide minerals at circumneutral pH. A drop in pH would thus be expected to

Table 6
Estimated solute flows, mineral weathering rates, mineral contents and mineral lifetimes for the coal mine site at Black Clough

Solute flows			Mineral contents			Mineral weathering rates		Mineral lifetimes	
	Mol s^{-1}	Tonnes $year^{-1}$		Mol	kg		Moles s^{-1}		Years
SO_4^{2-}	0.14	437	Pyrite (total)	1.5×10^9	1.8×10^8	Pyrite	7.2×10^{-2}	Pyrite	653
Ca^{2+}	9.5×10^{-2}	121	In coal	8.7×10^7	1.0×10^7	Calcite	9.5×10^{-2}	Calcite	532
Fe_T	3.3×10^{-2}	59	In mudstone	1.4×10^9	1.7×10^8				
			Calcite	1.6×10^9	1.6×10^8				

mobilise these contaminants through desorption or release of metal ions that are co-precipitated with the iron (hydr)oxide (compare Fig. 3).

3.3. The mill tailings impoundment 1 at Kristineberg, Sweden

3.3.1. Site description

The Kristineberg site, located approximately 120 km west of Skellefteå in the northern part of Sweden, has been mined for copper and zinc rich sulphidic ores since the 1940s. The enrichment plant, which was closed in 1991, received ore from the underground mine at the site and from other mines in the vicinity. There are five mill tailings impoundments and a small waste rock heap at the site (Fig. 6), but today no deposition of mine tailings or waste rock takes place over ground.

In the mid 1990s, Boliden Mineral AB, who owns and operates the site, initiated remediation of the site. The remediation followed the outcome of a programme for assessing protective measures after mining activities, and implies application of dry covers and a raised groundwater level (Impoundments 1B, 1, 2 and 3) as well as application of wet cover (Impoundments 2, 3 and 4) (Lindvall et al., 1999). This case study, which is based on previously reported field observations, assesses the Impoundment 1, which was in use from the 1940s to the 1950s, for the situation prior to remediation and provides results that can be compared to those of presently ongoing field studies (see e.g. MiMi (1999)).

Prior to remediation, the average groundwater level in Impoundment 1 was approximately 1 m with a seasonal variation of 1 m due to recharge events mainly at snowmelt during spring and at autumn rain. Drainage water discharged mainly to the surrounding ditches but fracture zones underlying the impoundment likely drained 10–14% of the leachate volume (Axelsson et al., 1986).

The tailings consist of a finely ground material (characterised as silty fine sand or fine sand) in

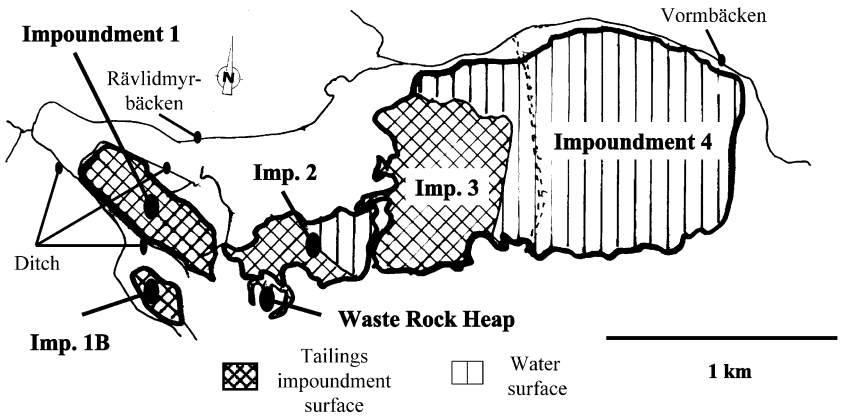

Fig. 6. Map over the Kristineberg site showing the impoundments with surroundings (modified from Boliden Mineral (1995)).

Table 7
Physical, mineralogical and chemical characteristics of the tailings and groundwater in Impoundment 1 at the Kristineberg site (Data from Qvarfort (1983), Axelsson et al. (1986), Qvarfort and Ekstav (1989), and others as compiled by Malmström et al. (2000b))

Physical data		Hydrological data		Chemical composition of tailings				Groundwater quality[a]	
						Unweathered zone (wt% element)	Weathered zone[b] (wt% element)		
Areal extent	1.1×10^5 m^2	Precipitation	660 mm year^{-1}					pH	5.01 ± 0.24
Depth total (average)	5 m	Water flow		S	(Pyrite, chalcopyrite, sphalerite)	13.0	7.6	SO_4^{2-}	9156 ± 2622 (mg l^{-1})
Weathered zone (average)	1 m	Discharge	43 000–54 000 m^3 year^{-1}	Fe[c]	(Pyrite)	9.5	4.8	Fe_{Tot}	3981 ± 960 (mg l^{-1})
Groundwater level (average)	1 m	Recharge	31 000–51 000 m^3 year^{-1}	Cu	(Chalcopyrite)	0.12	0.08	Cu^{2+}	2.71 ± 1.04 (mg l^{-1})
Temperature (annual average)	0.7°C	Water residence time		Zn	(Sphalerite)	1.1	0.61	Zn^{2+}	304 ± 155 (mg l^{-1})
Porosity	0.25	Unsaturated zone	0.5–1 years	Ca	(Calcite)	0.84	0.56	Ca^{2+}	253 ± 148 (mg l^{-1})
Compact density (tailings)[d]	3300 kg m^{-3}	Saturated zone	2–3 years	Mg	(Talc, chlorite, dolomite)	3.8	4.8	Mg^{2+}	246 ± 67 (mg l^{-1})
Specific surface area of tailings	0.1 m^2 g^{-1}								

[a] Average of annual mean values for all sampling locations and depths.
[b] Estimated as the arithmetic mean of the average content in the two uppermost samples in the weathered zone and the average content in the unweathered zone at each sample location.
[c] Iron bound in sulphide minerals. An additional 6.2 wt% Fe is bound in non-sulphide minerals.
[d] Compact density as estimated from mineralogy (Malmström et al., 2000b). In the calculations in the present study, representative compact mineral densities of sulphide and silicate minerals of 5100 and 2700 kg m^{-3}, respectively, were used.

which the main sulphides are pyrite, sphalerite, and chalcopyrite. The main carbonates are reportedly dolomite and calcite (~10 vol.% of the gangue material in the mine), and major silicates are quartz (~25 vol.%), muscovite (~15 vol.%) and magnesium phyllosilicates (talc and chlorite, ~50 vol.%; Qvarfort, 1983). The upper part of the impoundment, on average down to the groundwater level, had been partly depleted in sulphur, iron, zinc and copper (Table 7; Qvarfort, 1983). This is presumably the effect of oxidative weathering of sulphides in the unsaturated zone where oxygen diffusion likely has provided significant amounts of oxidants over the years.

The groundwater in impoundment 1, which during two years was sampled at several different locations at a depth of 1.5 and 7 m below the groundwater table, contained high concentrations of sulphate, iron, zinc, calcium and magnesium (see Table 7; data from Qvarfort and Ekstav (1989)). The concentrations of dissolved ions varied between the sampling locations and depths and over the year, however, the variation over time and between locations was larger than that between the two sampling depths. The average pH of 5.0 and the reported Mg^{2+} and Ca^{2+} concentrations indicate that the groundwaters are undersaturated with respect to calcite and dolomite.

3.3.2. Site assessment

To estimate the solute flows from Impoundment 1, we use the average annual water flow through the impoundment ($47\,000 \pm 4000\ m^3\ year^{-1}$) and the time averaged groundwater composition for available sample locations (Table 7). This approach assesses the total water discharge to both the surrounding ditches and underlying fracture zones and hence yields an estimate of the integrated contaminant export rate.

The solute mass balance of Impoundment 1 may be affected by surface water run off and groundwater recharge from Impoundment 1B that is situated upstream of Impoundment 1 (Fig. 6). However, as Impoundment 1B is small and was separated from Impoundment 1 by ditches, we, as a first approximation, do not regard any external sources of contaminants (see Malmström et al. (2000b), for a detailed discussion).

In order to estimate the present integrated mineral weathering rates, we use the calculated solute flows. As no other minerals release zinc and copper, estimates of the dissolution rates of sphalerite, R_{sph}, and chalcopyrite, R_{chp}, are directly obtained from the zinc and copper flows (compare Reactions d and e in Table 1 and Eq. (2))

$$R_{sph} = F_{Zn^{2+}} \qquad (mol\ s^{-1}) \tag{15}$$

$$R_{chp} = F_{Cu^{2+}} \qquad (mol\ s^{-1}) \tag{16}$$

We estimate the pyrite weathering rate, R_{pyr}, using the flow of both sulphate and iron. In both cases, the flow must be corrected for contributions of solutes from other sulphides and the stoichiometries of the reactions (Reactions a, e and f in Table 1)

$$R_{pyr}^{SO_4^{2-}} = \frac{(F_{SO_4^{2-}} - 2R_{chp} - R_{sph})}{2} = \frac{(F_{SO_4^{2-}} - 2F_{Cu^{2+}} - F_{Zn^{2+}})}{2} \quad (mol\ s^{-1}) \tag{17}$$

$$R_{pyr}^{Fe} = (F_{Fe} - R_{chp}) = (F_{Fe} - F_{Cu^{2+}}) \qquad (mol\ s^{-1}) \tag{18}$$

Assuming that all Ca^{2+} originates from carbonates (calcite or dolomite), we test two limiting cases where Ca^{2+} alternatively is assumed to originate from calcite and dolomite and estimate the corresponding weathering rates, R_{cal} and R_{dol}, as

$$R_{cal} = F_{Ca^{2+}} \qquad (mol\ s^{-1}) \tag{19a}$$

$$R_{dol} = F_{Ca^{2+}} \tag{19b}$$

(compare Reactions g–j in Table 1).

Because a key component in the gangue material is Mg-silicates (talc and chlorite) and high aluminium concentrations, indicative of extensive aluminiumsilicate weathering, are observed (not shown), we do not use Mg^{2+} as a tracer for dolomite weathering. The fact that the depth of the observed weathered zone coincides with the groundwater level and that the solute-concentrations do not significantly increase with depth below the groundwater table indicate that the source of solutes is likely the weathering of minerals in the zone above the groundwater table. This suggests that oxygen is mainly supplied to the unsaturated zone, as would be expected for diffusive

oxygen transport, characterised by more rapid transport in unsaturated pores. This implies that, due to much slower oxygen diffusion at saturated conditions, the main source of contaminants is the unsaturated zone. This is consistent with the observed depletion of e.g. in sulphur, iron, zinc and copper in this part of the impoundment (Table 7; Qvarfort, 1983). Moreover, this implies that the contaminant release rate will be drastically diminished when the sulphides have been fully depleted from the weathered zone above the groundwater table.

The mineralogical composition at the site was estimated from reported chemical composition of the tailings and the mineralogical composition of the ore and gangue material in the mine. Using Eq. (4b), we calculate the molar amount of minerals available for weathering using the areal extent of the impoundment and the average depth and chemical composition of the weathered zone (Table 7). With the exception of using sulphur instead of sulphate, we use the same mineral tracers and analogous corrections for the presence of other minerals and mineral stoichiometries as in the calculations of the mineral weathering rates (Eqs. (15)–(19b)). Through Eq. (3) we obtain the mineral lifetimes from the estimated weathering rates and the amounts of available minerals.

In mill tailings deposits, where oxygen transport is much slower than in waste rock heaps, oxygen transport (often dominated by diffusion, see e.g. Werner and Berglund (1999)) may be slower than the chemical kinetics and, hence, limit the sulphide weathering. Because diffusion-controlled and reaction-controlled kinetics exhibit different time-dependence, refinement of predictions for mineral lifetimes requires a correctly conceptualised dynamic model. In order assess the rate limiting process, we estimate an apparent diffusion coefficient and an apparent surface area normalised reaction rate, alternatively assuming a diffusion-controlled and a reaction-controlled mechanism.

We estimate the apparent surface area normalised reaction rate according to

$$r_{\mathrm{pyr}} = \frac{R_{\mathrm{pyr}}}{a_{\mathrm{s}} m_{\mathrm{TOT}} \gamma_{\mathrm{pyr}}} \qquad (\mathrm{mol\ m^{-2}\ s^{-1}}) \tag{20}$$

where a_{s} is the total specific surface area; m_{TOT} is the total mass of minerals in the weathered zone; and γ_{pyr} is the volume fraction of pyrite in the zone (γ_{pyr} is estimated to 6.5–8.8 vol.% from the chemical composition listed in Table 7).

We calculate the areal oxygen flux, $f_{\mathrm{O_2}} = F_{\mathrm{O_2}}/A$, using the sulphide weathering rates, the areal extent of the impoundment and the stoichiometric coefficients that relate pyrite, sphalerite and chalcopyrite weathering to oxygen consumption (see Reactions a, d, e and f in Table 1) according to

$$f_{\mathrm{O_2}} = \frac{(7/2)R_{\mathrm{pyr}} + 2R_{\mathrm{sph}} + 4R_{\mathrm{chp}}}{A} \qquad (\mathrm{mol\ m^{2}\ s^{-1}}) \tag{21}$$

Using the areal oxygen flux, we estimate an apparent effective diffusion coefficient, D_{e}, by solving Fick's law

$$f_{\mathrm{O_2}} = \frac{D_{\mathrm{e}} \Delta C}{z} \qquad (\mathrm{mol\ m^{2}\ s^{-1}}) \tag{22}$$

at an oxygen gradient, ΔC, of 9.3 mol $\mathrm{m^{-3}}$ and a diffusion length, z, of 1 m. This condition corresponds to atmospheric concentration of oxygen at the impoundment surface, full oxygen depletion at the interface between the saturated and unsaturated zone, steady-state reaction kinetics and no further reaction below a depth of 1 m.

We do not imply that we can make actual parameter estimates for the effective diffusion coefficient and the surface area normalised reaction rate of pyrite through Eqs. (22) and (20), respectively. The obtained values, however, can be compared to those previously reported in the literature in order to exclude either the oxygen diffusion or the surface reaction as the rate limiting step in the pyrite oxidation process.

3.3.3. Results and implications

Table 8 lists the calculated solute flows, the associated mineral weathering rates, the mineral contents in the weathered (unsaturated) zone and the estimated lifetimes of the minerals in this zone. In agreement with previously published results, which were based on surface water flows and qualities in dams surrounding the impoundment (Qvarfort and Ekstav, 1989), our estimated solute flows indicate a considerable contaminant export prior to remediation. Attenuation and accumulation of the contaminants have likely occurred in the downstream Impoundments 2–4.

Table 8
Estimated solute flows, mineral weathering rates, mineral contents and mineral lifetimes for the unsaturated, weathered zone in Impoundment 1 in Kristineberg

Solute flows			Mineral contents			Mineral weathering rates		Mineral lifetimes	
	Mol s^{-1}	Tonnes $year^{-1}$		Mol	kg		Mol s^{-1}		Years
Fe_{Tot}	0.11	187	Pyrite (based on Fe)	2.3×10^{8}	2.8×10^{7}	Pyrite (based on Fe flow)	0.11	Pyrite (based on Fe)	69
SO_4^{2-}	0.14	430	based on S	3.1×10^{8}	3.7×10^{7}	based on SO_4^{2-} flow	6.8×10^{-2}	based on S and SO_4^{2-}	144
Cu^{2+}	6.4×10^{-5}	0.13	Chalcopyrite	3.4×10^{6}	6.3×10^{5}	Chalcopyrite	6.4×10^{-5}	Chalcopyrite	1710
Zn^{2}	6.9×10^{-3}	14	Sphalerite	2.5×10^{5}	2.5×10^{6}	Sphalerite	6.9×10^{-3}	Sphalerite	116
Ca^{2+}	9.4×10^{-3}	12	Calcite	3.8×10^{7}	3.8×10^{6}	Calcite/dolomite	9.4×10^{-3}	Calcite/dolomite	(128)[a]

[a] Other sources/sinks for Ca^{2+} are plausible.

The estimates of the lifetime for pyrite and sphalerite in the unsaturated zone are on the orders of 100 years. The discrepancy between the estimated lifetime for pyrite based on the iron and the sulphate flows may be the result of additional processes affecting the flows, e.g. immobilisation of sulphate through gypsum precipitation (resulting in an overestimation of the pyrite lifetime) or mobilisation of iron through chlorite weathering and/or oxidation of pyrite by ferric iron (resulting in an underestimation of the pyrite lifetime). Our estimates, which hence may frame a lower and an upper limit for the pyrite lifetime, show a contaminant source duration on the order of 100 years. This implies the need for long-term remediation measures. The owner has applied dry cover to the impoundment (Lindvall et al., 1999).

The estimated lifetime of chalcopyrite is on the order of thousands of years. The much longer apparent lifetime of chalcopyrite than of pyrite may indicate immobilisation of Cu^{2+} due to adsorption reactions or precipitation of secondary Cu minerals in or below the weathered zone. Release of the accumulated copper due to decrease in pH after calcite is consumed or due to increased oxygen level after pyrite is depleted may cause a temporarily increased copper flow at that point (compare Fig. 3).

The calcite/dolomite lifetime is estimated to be on the order of 100 years. This suggests that the impoundment would stay buffered over large parts of the contaminant duration. However, based on the reported carbonate content of the tailings, it has been speculated that only a part of the calcium content is bound in carbonates (Malmström et al., 2000b). In fact, the average measured pH of about five shows that calcite/dolomite does not reach solubility equilibrium. This may indicate that available calcite/dolomite already has been depleted and that other processes than carbonate mineral weathering are responsible for the pH buffering and for the calcium release. This is consistent with the reported negative net neutralising potential (NNP) of the tailings (-500–0 kg $CaCO_3$ tonne^{-1}; Jönsson, 1992). The weathering of Mg-silicates, such as talc and chlorite, which are abundant minerals in the tailings is a plausible process for acidity consumption in the absence of carbonates and may also contribute to the high concentrations of Mg^{2+} and Al^{3+} found in the groundwater. In a more detailed model, the weathering of pyrite, chlorite and a secondary Fe(III)-hydroxide was suggested to explain the proton balance at the site (Salmon and Malmström, 2000).

In mill tailings deposits, either oxygen diffusion or (bio)geochemical kinetics may limit the sulphide weathering rate. In order to assess the rate-limiting step, we alternatively assumed (bio)geochemical kinetic control and diffusion control of the process. We estimated the apparent surface area normalised pyrite weathering rate and the apparent effective diffusion coefficient in the unsaturated zone, respectively, and compared the estimated values to those reported in the literature. An apparent surface area normalised pyrite weathering rate much lower than those reported in the literature would indicate that the oxidation process is limited by diffusion. On the other hand, an apparent effective diffusion coefficient much lower than those reported in the literature would exclude diffusion controlled oxidation and indicate a (bio)geochemically controlled oxidation process.

Using Eq. (20), we estimated an apparent surface area normalised pyrite weathering rate of $(2.3\text{–}4.8) \times 10^{-11}$ mol m^{-2} s^{-1} which is one order of magnitude lower than that reported for reaction controlled kinetics determined in laboratory experiments at 25°C; $2 < \text{pH} < 8$ and $PO_2 = 0.2$ atm (Strömberg and Banwart, 1994, citing personal communication from R. Nicholson). This is consistent with the fact that mineral weathering rates normally show a large scale-dependence with one to three orders of magnitude lower rates in the field as compared to those in laboratory experiments for reasons other than diffusion rate control (Malmström et al., 2000a).

We calculated an areal oxygen flux of $(2.3\text{–}3.5) \times 10^{-6}$ mol O_2 m^{-2} s^{-1} from which we derived an effective diffusion coefficient of $(2.4\text{–}3.8) \times 10^{-7}$ m^2 s^{-1} (Eq. (22)). This diffusion coefficient value is comparable to those determined for other mill tailings samples in laboratory experiments (compare Nicholson et al. (1989)).We thus conclude that estimates of the apparent surface area normalised reaction rate and the apparent effective oxygen diffusion coefficient are comparable to those reported in the literature. Hence, based on available data, neither the kinetic-controlled nor the diffusion-controlled mechanism can be rejected. It appears that an appropriate conceptual model for the weathering

must assess mixed kinetics. Determination and analysis of oxygen concentration profiles in the impoundment can further test this hypothesis.

4. Discussion and conclusions

4.1. Sources of error

For the stated objectives of preliminary hydrochemical modelling, the key step in model development is the conceptualisation of possible transport and reaction processes. This leads to formulation of simple mathematical expressions for solute flows and process rates that allow estimates of contaminating lifetimes and potential evolution of discharge quality. The main value of developing the model is not a prediction of pollution loads, but rather a scientifically-based analysis that forces investigators to think carefully about what can be happening at a site, and how it will impact environmental risk. The key errors that can occur in such modelling are thus conceptual errors where dominant processes at a site are not included in the preliminary model. There are a number of checks that can be subsequently carried out to test assumptions upon which the model is based. The framework presented above provides a list of reactive and transport processes that can be evaluated in the first instance for a site, and then checked against additional data if available.

For advective transport processes, the water flows that are used to calculate solute flows can be checked against a water balance for a site. Gross errors, such as failing to take note of a significant recharge area or discharge point at a site, can thus be checked. The point estimates of water flows and solute concentrations used in the preliminary model may not be representative regarding the temporal variability in water and solute flows. Immobile water can be assumed to play a role in many subsurface systems, although quantifying the impact is difficult in the absence of results from unreactive tracer tests.

Additional reaction processes that can impact the hydrochemical modelling presented above are any processes that affect a discharge regarding the amounts and ratios of solute ion concentrations that arise from weathering processes. Important processes are solute immobilisation reactions such as secondary mineral formation and metal ion adsorption that remove solutes from solution. Also, solid phase transformations of minerals that alter the apparent stoichiometry of a weathering reaction, for example formation of covellite (CuS(s)) from pyrrhotite (FeS(s)), may affect model results.

Calculating mineral weathering rates from solute flows relies on knowing the mineralogy at a site, and the mineral chemistry; i.e. the composition of the minerals present. For an estimate of the molar amount of the minerals also the relative abundance of the minerals needs to be known. For the Black Clough site, values were taken from handbooks on mining geology and from standard mining records. For Kristineberg, the mineralogical composition at the site was estimated from reported chemical composition of the tailings and the mineralogical composition of the ore and gangue material in the mine. For Aitik, drill cores were quantitatively characterised by thin-section microscopy and mineral chemical analysis.

4.2. Building on the preliminary model results

Additional data to address potential errors regarding the processes to be included in the model include checking the water balance, measuring flow rates and obtaining meteorological data if necessary. Groundwater flows and associated solute flows can be better determined if monitoring data including groundwater heads and groundwater quality are available. Reaction rates can be determined by alternative methods, primarily oxygen consumption measurements in packed-off boreholes. Gas transport rates, for example into tailings deposits, can be estimated from oxygen profiles. Such profiles may also help to discriminate between oxygen transport limitation and a (bio)geochemical limitation of the sulfide oxidation rate. Mineralogical investigations; sampling and quantitative analysis of mineral abundance and mineral chemistry, can constrain the possible stoichimetry used when calculating weathering rates from solute flows.

Additional modelling can be carried out if a suitable database exists or is developed through subsequent site investigations. For example, the possibility of secondary mineral formation can be checked against geochemical modelling of aqueous speciation. This

allows the saturation state of an aqueous sample to be assessed with respect to possible secondary minerals. Gross undersaturation can infer that the mineral is unlikely to form. Such conclusions can be checked against the results of mineralogical investigations; i.e. are such minerals observed?

The processes discussed in this section, and the nature of data required to better quantify them, is not considered to be an exhaustive list. It serves to point out that the extent of site investigation and site modelling depends directly on the level of detail required in site understanding to make an acceptable risk management decision.

4.3. Environmental decision making

We have attempted to outline a relatively simple hydrochemical modelling approach for preliminary assessment of minewater pollution. Within the source–pathway–target framework for risk assessment, this corresponds to source-term modelling for sulphide mineral weathering, and attenuation of acidity by calcite and aluminosilicate weathering reactions with the associated immobilisation of heavy metal ions along advective transport pathways to sensitive targets such as receiving streams. The method is not data intensive, and can be carried out as a desk study based on limited hydrochemical and hydrological data and information provided in mining records.

Based on the results presented in the above case studies, two points are to be emphasised regardless of the extent of site investigation and site modelling that is carried out. First, the longevity of contamination is critical to risk management decisions. It is beyond the scope of this study to exhaustively describe treatment and remediation technologies for minewater pollution. Younger (1997) has provided an excellent guide to potential treatment options, and decision-making that considers contamination longevity. In short, contamination on the scale of decades can be treated with active methods such as chemical addition; e.g. lime dosing to treat acidic discharges. Contamination on longer time scales cannot rely on the maintenance and performance of engineered structures and the continuity of regulatory control. In this case, treatment requires passive schemes such as cover layers to prevent oxygen ingress, capping to prevent infiltration or constructed wetlands to treat aqueous discharges.

Second, contamination water quality can change. Remediation schemes for alkaline discharges may be confronted with acidic discharges if the natural acidity attenuation capacity provided by carbonate minerals such as calcite becomes depleted. In this case, even if the treatment scheme performs well initially, it may not be able to adequately treat the future water quality.

Although additional site investigations and additional analysis via model development and application can continue indefinitely, the resulting certainty in the understanding of the site and the risk it presents must be balanced against the time and financial cost of additional analysis. The modelling presented above is considered to be consistent with a Tier 1 approach to aid risk assessment. If the analysis suggests that the site represents significant risk and that major capital expenditure is required to manage the risk, then a second-tier of site investigation and modelling may be required. The savings in optimising the remediation and/or monitoring concept, based on results from the second-tier assessment, may justify the additional investigations.

The intention of the preliminary assessment framework outlined above is thus to help understand the site. This includes demonstrating potential controls on contamination loads and their longevity and predicting possible future changes in water quality. We advocate this quantitative approach in order to help assess monitoring requirements, and to prioritise any future investigations that may required to reduce uncertainty in subsequent risk assessment and decision making.

Acknowledgements

This research was funded by the Swedish Foundation for Strategic Environmental Research (MISTRA) through the research programme ‘Mitigation of the environmental impact from mining waste’ (MiMi). We wish to acknowledge collaborative links at U. Sheffield with project GST/02/2060 of the Natural Environment Research Council (UK), Environmental Diagnostics programme. Site data for the Black Clough discharge were provided by the Environment Agency of England and Wales.

References

Alpers, C.N., Nordstrom, D.K., 1999. Geochemical modeling of water-rock nteractions in mining environments. Rev. Econ. Geol. 6A, 289–323.

ASTM, 1996. ASTM Designation: D 5744-96 — Standard Test Method for Accelerated Weathering of Solid Materials Using a Modified Humidy Cell. American Society for Testing and Materials, West Conshohocken, PA.

ASTM, 1995. Designation: E 1739-95 — Guide to Risk-Based Corrective Action at Petroleum Release Site. American Society for Testing and Materials, West Conshohocken, Pennsylvania.

Axelsson, C.-L., Karlqvist, L., Lintu, Y., Olsson, T., 1986. Gruvindustrins restproduktupplag — fältundersökningar med vattenbalansstudie i Kristineberg, Uppsala Geosystem AB, Sweden, 1986, in Swedish, with summary in English.

Axelsson, C.L., Byström, J., Holmén, J., Jansson, T., 1992. Efterbehandling av sandmagasin och gråbergsupplag i Aitik, Hydrogeologiska förutsättningar för åtgärdsplan. Golder Geosystem, AB., Report 927-1801, in Swedish.

Boliden Mineral, 1995. Utredningar avseende efterbehandlingsåtgärder. Kristineberg Magasin 1 och 2. Boliden Mineral, AB., Sweden, in Swedish.

Capewell, S., 1996. Environmental Assessment of Mine Water Pollution. Undergraduate Dissertation, Dept. of Civil and Environmental Engineering, University of Bradford (UK).

Chou, L., Garrels, R.M., Wollast, R., 1989. Comparative study of the kinetics and mechanisms of dissolution of carbonate minerals. Chem. Geol. 78, 269–282.

Eriksson, N., 1996. Coupling hydrological and chemical processes that affect filed-scale metal leaching from mining waste rock. Licentiate thesis, Division of Water Resources Engineering, Royal Institute of Technology, Stockholm.

Eriksson, N., Gupta, A., Destouni, G., 1997. Comparative analysis of laboratory and field tracer tests for investigating preferential flow and transport in mining waste rock. J. Hydrol. 194, 143–163.

Evans, J.W., 1979. Mass transfer within chemical reactions. Miner. Sci. Engng. 11, 207–223.

Finkelman, R.B., Giffin, D.E., 1986. Hydrogen peroxide oxidation: an improved method for rapidly assessing acid-generation potential of sediments and sedimentary rocks. Recl. Reveg. Res. 5, 521–534.

Gautelier, M., Oelkers, E.H., Schott, J., 1999. An experimental study of dolomite dissolution rates as a function of pH from −0.5 to 5 and temperature from 25 to 80°C. Chem. Geol. 157, 13–26.

Jönsson, H., 1992. Efterbehandlingsprojekt — Kristineberg: Provtagning av Magasin 1, 1B och 2. Boliden Miner. AB, in Swedish.

Kwong, Y.T., Ferguson, K.D., 1997. Mineralogical changes during NP determinations and their implications. Proc. 4th Conf. Acid Rock Drainage, May 31–June 6, 1997, Vancouver, BC, Canada, vol. 1, pp. 435–447.

Lawrence, R.W., Wang, Y., 1997. Determination of neutralization potential for acid rock drainage prediction. Natural Resources Canada, CANMET, MEND report 1.16.3.

Li, M.G., 1997. Neutralization potential versus observed mineral dissolution in humidity cell tests for Louvicourt tailings. Proc. 4th Conf. Acid Rock Drainage, May 31–June 6, 1997, Vancouver, BC, Canada, vol. 1, pp. 149–164.

Lindvall, M., Eriksson, N., Ljungberg, J., 1999. Decommissioning at Kristineberg mine, Sweden. Proceeding Sudbury'99 Mining and the Environment II, 13–17 Sept. 1999, Sudbury, Ontario, Canada, pp. 855–862.

Malmström, M.E., Destouni, G., Banwart, S.A., Strömberg, B.H.E., 2000a. Resolving the scale-dependence of mineral weathering rates. Environ. Sci. Technol. 34 (7), 1375–1378.

Malmström, M., Werner, K., Salmon, S., Berglund, S., 2000b. Hydrogeology and geochemistry of mill tailings impoundment 1, Kristineberg, Sweden: Compilation and interpretation of pre-remediation data. MiMi-report, MISTRA Research Programme: Mitigation of the Environmental Impact from Mining Waste, Stockholm, Sweden, in print.

MiMi, 1999. Moräntäckning som efterbehandlingsmetod av gruvavfall. In: Årsrapport 1998 för MISTRA-programmet MiMi åtgärder mot miljöproblem från gruvavfall. MiMi-Report, MISTRA Research Programme: Mitigation of the Environmental Impact from Mining Waste, Stockholm, Sweden, in Swedish.

Nicholson, R.V., Gilham, R.W., Cherry, J.A., Reardon, E.J., 1989. Reduction of acid generation in mine tailings through the use of moisture-retaining cover layers as oxygen barriers. Can. Geotechnol. 26, 1–8.

O'Shay, T., Hossner, L.R., Dixon, J.B., 1990. A modified hydrogen peroxide oxidation method for determination of potential acidity in pyritic overburden. J. Environ. Qual. 19 (4), 778–782.

Paktunc, A.D., 1999a. Characterization of mine wastes for prediction of acid mine drainage. In: Azcue, J.M. (Ed.), Environmental Impacts of Mining Activites. Springer, Germany, pp. 19–40.

Paktunc, A.D., 1999b. Mineralogical constraints on the determination of neutralizing potential and prediction of acid mine drainage. Environ. Geol. 39, 103–112.

Perkins, E.H., Nesbitt, H.W., St-Arnaud, L.C., 1997. Critical review of classes of geochemical computer models adaptable for prediction of acidic drainage from mine waste rock. Fourth Int. Conf. Acid Rock Drainage, May 31–June 6 1997, Vancouver, BC, Canada, vol. II, pp. 587–601.

Price, W.A., 1997. DRAFT guidelines and recommended methods for the prediction of metal leaching and acid rock drainage at minesites in British Columbia. British Columbia Ministry of Employment and Investment, Energy and Minerals Division, Smithers, BC.

Qvarfort, U., 1983. En kartläggning av sandmagasin från sulfidmalmsbrytning. Naturvårdsverkets Rapport SNV PM 1699, Sweden, in Swedish.

Qvarfort, U., Ekstav, A., 1989. Metallbalans Kristineberg. Report Kvartärgeologiska avdelning at Uppsala Universitet, Sweden, in Swedish.

Salmon, U.J., Malmström, M.E., 2000. Modelling of mill tailings impoundment geochemistry and remediation. Proc. 6th Int. Conf. Appl. Min., ICAM2000, 17–19 July 2000, Göttingen, Germany, vol. 2, pp. 671–673.

Scharer, J.M., Nicholson, R.V., Halbert, B., Snodgrass, W.J., 1994. A computer programme to assess acid generation in pyritic

tailings. In: Alpers, C.N., Blowes, D.W. (Eds.), Environmental Geochemistry of Sulfide Oxidation. ACS Symposium Series 550. The American Chemical Society, Washington, DC, pp. 132–152.

Sobek, A.A., Schuller, W.A., Freeman, J.R., Smith, R.M., 1978. Field and laboratory methods applicable to overburdens and minesoils. US EPA publ. EPA-600/2-78-054.

Strömberg, B., 1997. Weathering kinetics of sulphidic mining waste: An assessment of geochemical processes in the Aitik mining waste rock deposits. PhD-thesis, Department of Chemistry, Division of Inorganic Chemistry, Royal Institute of Technology, Stockholm.

Strömberg, B., Banwart, S., 1994. Kinetic modelling of geochemical processes at the Aitik mining waste rock site in northern Sweden. Appl. Geochem. 9, 583–595.

Strömberg, B., Banwart, S., 1999a. Experimental study of acidity consuming processes in mining waste rock: Some influences of mineralogy and particle size. Appl. Geochem. 14, 1–16.

Strömberg, B., Banwart, S., 1999b. Weathering kinetics of waste rock from the Aitik copper mine, Sweden: scale dependent rate factors and pH controls in large column experiments. J. Cont. Hydrol. 39, 59–89.

Sverdrup, H.U., 1990. The kinetics of base cation release due to chemical weathering. Lund Univ. Press, Sweden, 246 p.

Werner, K., Berglund, S., 1999. Effects of spatial variability on oxygen transport in sulphidic mining waste deposits, Sudbury'99. Mining and the Environment II, 13–17 Sept. 1999, Sudbury, Canada, pp. 243–252.

White, W.W., Jeffers, T.H., 1994. Chemical predictive modelling of acid mine drainage from metallic sulfide-bearing waste rock. In: Alpers, C.N., Blowes, D.W. (Eds.), Environmental Geochemistry of Sulfide Oxidation. ACS Symp. Ser. 550, pp. 608–630.

White, A.F., Brantley, S.L., 1995. Chemical weathering rates of silicate minerals. Rev. Mineral. 31 Am. Min. Soc.

White, W.W., Lapakko, K.A., Cox, R.L., 1999. Static-test methods most commonly used to predict acid-mine drainage: practical guidelines for use and interpretation. Rev. Econ. Geol. 6A, 325–338.

Williamson, M.A., Rimstidt, J.D., 1994. The kinetics and electrochemical rate-determining step of aqueous pyrite oxidation. Geochim. Cosmochim. Acta 58, 5443–5545.

Younger, P.L., 1997. The longevity of minewater pollution: a basis for decision-making. Sci. Tot. Environ. 194/195, 457–466.